Available online at www.sciencedirect.com
SCIENCE DIRECT®
Journal of Solid State Chemistry 177 (2004) 3131–3139
JOURNAL OF SOLID STATE CHEMISTRY
http://elsevier.com/locate/jssc

Structure, stoichiometry and magnetic properties of the low-dimensional structure phase $LiCuVO_4$

A.V. Prokofiev,[a,*] I.G. Vasilyeva,[b] V.N. Ikorskii,[b] V.V. Malakhov,[c] I.P. Asanov,[d] and W. Assmus[a]

[a] *Physikalisches Institut, J.W. Goethe Universität, 60054 Frankfurt a.M., Germany*
[b] *Nikolaev Institute of Inorganic Chemistry, SB of RAS, Novosibirsk 630090, Russia*
[c] *Boreskov Institute of Catalysis, SB of RAS, Novosibirsk 630090, Russia*
[d] *Samsung Advanced Institute of Technology, P.O. Box 111, Suwon 440-600, South Korea*

Received 27 February 2004; accepted 17 May 2004

Available online 8 July 2004

Abstract

A systematic investigation of a series of single- and polycrystalline $LiCuVO_4$ samples by means of X-ray diffraction, X-ray photoelectron spectroscopy, differential dissolution analysis, and magnetic susceptibility measurement were performed. This study reveals a noticeable difference in stoichiometry and structure of the samples prepared in different ways. The magnetic properties are discussed with respect to phase inhomogeneity, non-stoichiometry and structural defects.

Keywords: Spin chain compound; Stoichiometry; Single crystals; Differential dissolution; XPS; Magnetic susceptibility

1. Introduction

$LiCuVO_4$ contains a network of chains of edge-sharing CuO_6 and LiO_6 octahedra running along *a* and *b* axes, respectively (Fig. 1) [1]. Quasi-one-dimensional short-range antiferromagnetic correlations along the CuO_6 octahedron chains and a weak inter-chain coupling resulting in a transition to the Neel state were found [2–5]. However, the magnetic properties and, especially, the low-temperature behavior of the magnetic susceptibility appear to depend upon the sample preparation conditions. The nature of the upturn of the magnetic susceptibility below 10 K, which is a manifestation of the deviation from the antiferromagnetic Heisenberg spin chain model, is not yet clear. Although it was briefly discussed in [2] both from the positions of possible paramagnetic impurities and of an intrinsic property of $LiCuVO_4$, the lack of experimental results about real stoichiometry and the real structure of this compound has not allowed a definite conclusion. In most studies the physical properties were measured without direct determination of the real stoichiometry, assuming that the stoichiometry was correctly given by nominal composition of the starting oxide mixture, if no impurity phases were found in the final product by XRD method.

A possibility of non-stoichiometry of the grown crystals was discussed in [7]. A slight excess of Cu ($Cu/V = 1.025 \pm 0.03$)—within the experimental error of the technique—was observed by EDXA which was, however, not able to determine the Li content. To investigate the influence of stoichiometry, a series of powder samples $Li_{1-x}CuVO_4$ ($0 < x < 0.2$) with composition fixed by appropriate proportions of the starting reagents was investigated in [6]. It was shown that the Li deficiency is compensated by non-Jahn–Teller ions Cu^{3+} in the Cu^{2+} sites, and in partial occupation of Li vacant sites by the Cu^{2+} ions.

This work presents a systematic investigation of $LiCuVO_4$ prepared by different techniques. It concerns

*Corresponding author. Physikalisches Institut, Johann Wolfgang Goethe Universität, Kristall- und Materialentwicklungslabor, Robert-Mayer-Strasse 2-4, DE-60325 Frankfurt am Main, 60054 Frankfurt a.M., Germany. Fax: +49-69-798-28520.
E-mail address: prokofiev@physik.uni-frankfurt.de (A.V. Prokofiev).

0022-4596/$ - see front matter © 2004 Elsevier Inc. All rights reserved.
doi:10.1016/j.jssc.2004.05.031

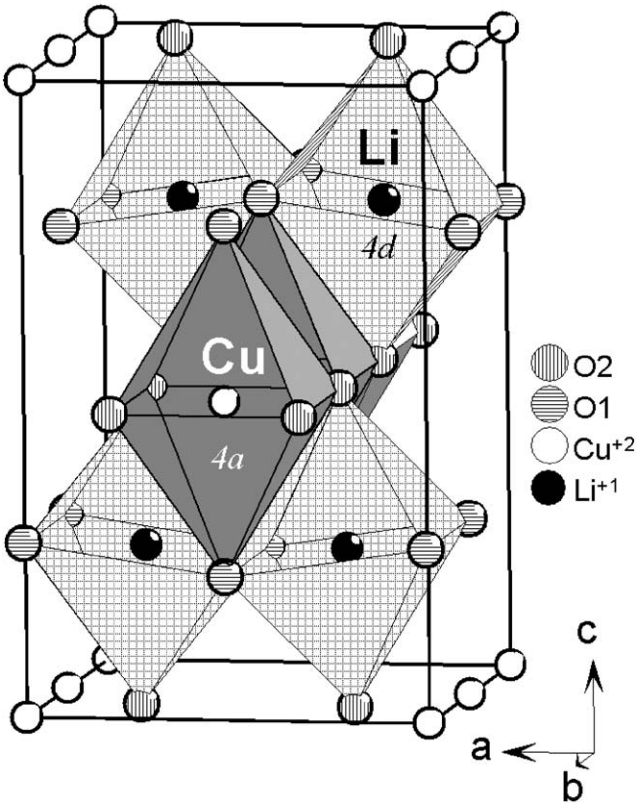

Fig. 1. Fragment of the $LiCuVO_4$ crystal structure with the unit cell edges [1]. Vanadium polyhedra are not shown.

a powder X-ray diffraction, a structural refinement using the single-crystal X-ray analysis, precise determination of real composition using differential dissolution technique in combination with ICP (differential dissolution analysis—DD), examination of the oxidation state of copper and vanadium using X-ray photoelectron spectroscopy (XPS), and measurement of the magnetic properties in the temperature range of 2–500 K.

2. Experimental

A series of five samples prepared by different techniques was taken for our study. Batches of single crystals of mm-scale size were grown from a solution of $LiCuVO_4$ in the $LiVO_3$–LiCl eutectics melt at 560–620°C (sample 1) and in the $LiVO_3$ melt at 650–680°C (sample 2), respectively. The growth details are given in [7]. Powder samples 3 and 4 of about 20 g were prepared by traditional solid-state reaction of appropriate mixtures of CuO, Li_2CO_3 and V_2O_5 at a temperature of 530°C during 10 days with seven intermediate grindings. The stoichiometric ratio of the reagents was taken for preparation of sample 3, and a mixture with a lack of Li_2CO_3 for sample 4. Sample 5 was prepared at a lower temperature (400°C). To avoid the low diffusion rate at this temperature, the preparation was carried out in a liquid flux in two stages. A partial dissolution of $LiVO_3$ in the eutectics RbCl–CuCl (m.p. 150°C) at 400°C in argon was followed by a slow increase in the oxygen concentration in the atmosphere. During this process, an oxidation of CuCl to CuO with simultaneous reaction between CuO and $LiVO_3$ in the flux takes place. The powder was washed by water to remove RbCl. All 1–5 samples were single phase according to powder XRD analysis.

Room temperature lattice parameters of powder samples were determined by the X-ray whole-pattern decomposition method. As internal standard, high-purity silicon powder was used ($a = 5.430940$ Å). Determination of crystal structure was performed for a single crystal grown from $LiVO_3$–LiCl eutectics using an Enraf-Nonius CAD-4 diffractometer.

Gross as well as local compositions of each thin layer removed by dissolution of samples (resolution about 1000 Å) were measured by the DD technique. Detailed description of the equipment and dissolution procedure of the technique is given in [8,9]. About 10 individual crystals of samples 1 and 2 or about 7 portions of powder samples 3–5 were analyzed. The weights were dissolved in 1 M HNO_3 and the contents of Li, Cu, and V were determined over the dissolution time in 300–500 solution portions. The kinetic curves of the Li, Cu, V dissolution and the stoichiograms, as molar ratios of Li/Cu, Cu/V, and Li/V, related to the same time-scale, were recorded. According to the main principles of DD, a horizontal linearity of stoichiograms during the whole dissolution process means a dissolution of an individual phase of a chemically homogeneous sample. In this case, the values of the stoichiograms correspond directly to the stoichiometric coefficients of the dissolved solid phase. Any local or extended deviation from the linearity of stoichiograms is an evidence of a chemical inhomogeneity of the sample. Basing on the main principles of DD, a set of rules was developed to interpret the origin of the observed deviations [8–10].

A Quantum 2000 Scanning ESCA Microprobe (Physical Electronics) spectrometer with monochromatic Al$K\alpha$ radiation ($h\nu = 1486.6$ eV) was used for the XPS study. The powder samples were pounded immediately before the measurement. To avoid the charging effect, a combined irradiation of slow electrons and of Ar+ ions was used. The spectra of the samples were recorded at room temperature and the binding energy (BE) values were measured relative to the position of the V $2p_{3/2}$ peak (517 eV). The relative concentration of the elements in all samples was estimated from the area of the peaks using sensitivity factors.

The magnetic susceptibility of the samples was measured in the temperature range of 2–300 K and in a magnetic field of 5 kOe using a Quantum design SQUID magnetometer. A diamagnetic contribution of

$LiCuVO_4$ ($-64\times10^{-6}\,cm^3/mol$) and χ_{TIP} Cu^{+2} ion ($60\times10^{-6}\,cm^3/mol$) were taken into account.

3. Results and discussion

3.1. Structural study

The XRD patterns of ground crystals and powders are shown in Fig. 2. For all samples, no additional lines that could be assigned to the presence of impurities were found. Samples 1–3 and 5 can be completely indexed with the orthorhombic crystal system with the space group *Imma*. The powder pattern of sample 4 shows a splitting of the (002), (112) (200) and (103) orthorhombic reflexes and this structure may be described well as a slightly distorted one. Contrary to samples 1 and 5, samples 2 and 3 show smearing of the (103), (121), (004), and (220) doublet reflexes, which results in some broadening and slight increasing of the unit-cell parameters of these samples (Table 1). The smaller the values of the lattice parameters, the higher the degree of the structural perfection of the samples. Crystals, grown from the eutectics (sample 1), are most perfect. A disorder appears in other samples, increasing in the sample range $5\rightarrow2\rightarrow3\rightarrow4$. A quite high background is

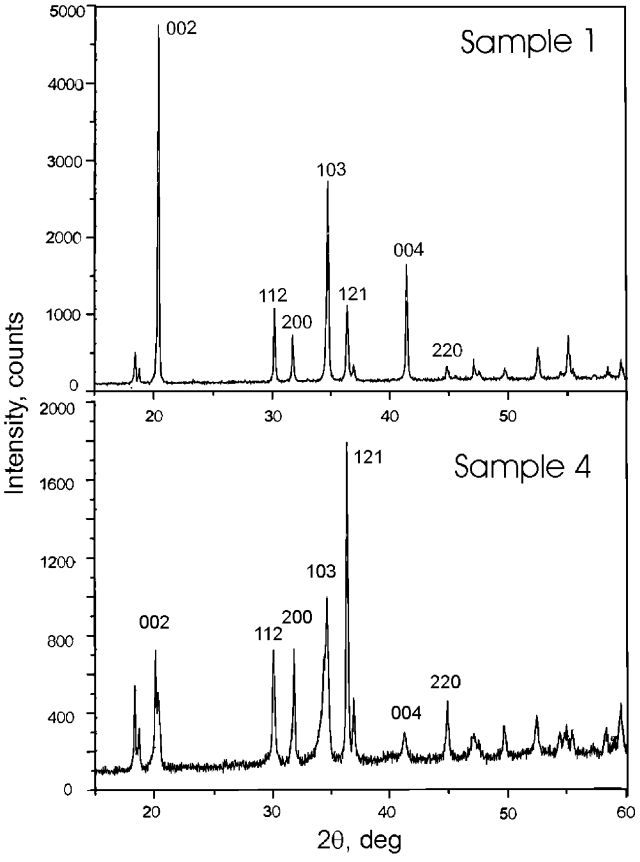

Fig. 2. The X-ray diffraction pattern of samples 1 and 4.

Table 1
Cell parameter c of the samples 1–5

Sample number	Parameter c (Å)
1	8.745
2	8.755
3	8.753
4	8.772
5	8.749

observed for powder samples 3 and 4 compared to the single-crystal samples, which may be an evidence of a phase inhomogeneity of the powders.

A special attention was given to the anomaly of intensities for (002), (121) and (400) reflexes of samples 1–3 and 5. This anomaly retains, in spite of the use of texture-eliminating procedures. The (002) reflex is anomalously high, whereas the (121) reflex is anomalously low, compared to the previously published data obtained from a structural refinement of a $LiCuVO_4$ single crystal grown by the hydrothermal method [1]. It should be noted that these are the reflexes that undergo also the most pronounced splitting in sample 4. Other authors also observed the over-distribution of the reflex intensities of powder $LiCuVO_4$ samples prepared by the standard solid-state reaction method [6,11,12]. Probably, the hydrothermal single crystal itself, being a reference, has anomalous intensities with regard to the samples prepared by the solid-state procedure. Therefore, we refined the crystal structure with a high-quality single crystal $LiCuVO_4$, grown from the $LiCl–LiVO_3$ eutectics. Detailed structural information will be published elsewhere. However, the intensity ratio of the reflexes as well as the refined atomic coordinates, composition and lattice parameters of our single crystal are very close to that of the hydrothermally grown one [1]. Our attempts to explain the observed anomalous intensity by an exchange of Li and Cu atoms between 4*a* and 4*d* sites or by a deficiency of Li, Cu, V, O without disruption of the initial lattice or by a slight displacement of atoms, lying closely to these planes, were powerless.

3.2. Composition study

Figs. 3 and 4 show kinetic curves of the Li, Cu, and V dissolution and the Li/Cu, V/Cu, and Cu/V stoichiograms of samples 1–5.

Stoichiometric $LiCuVO_4$ is characterized by a superposition of all the three kinetic curves (termed in mol/mL) and linear stoichiograms with the values equal to 1. The stoichiograms of such type with the values of $Li/Cu=0.99\pm0.02$, $Li/V=0.99\pm0.03$ and $Cu/V=1.00\pm0.01$ were observed only for some crystals of sample 1. Other crystals of the same batch were found to be slightly Li-deficient ($Li/V=0.99–0.95$) (Fig. 3a). The

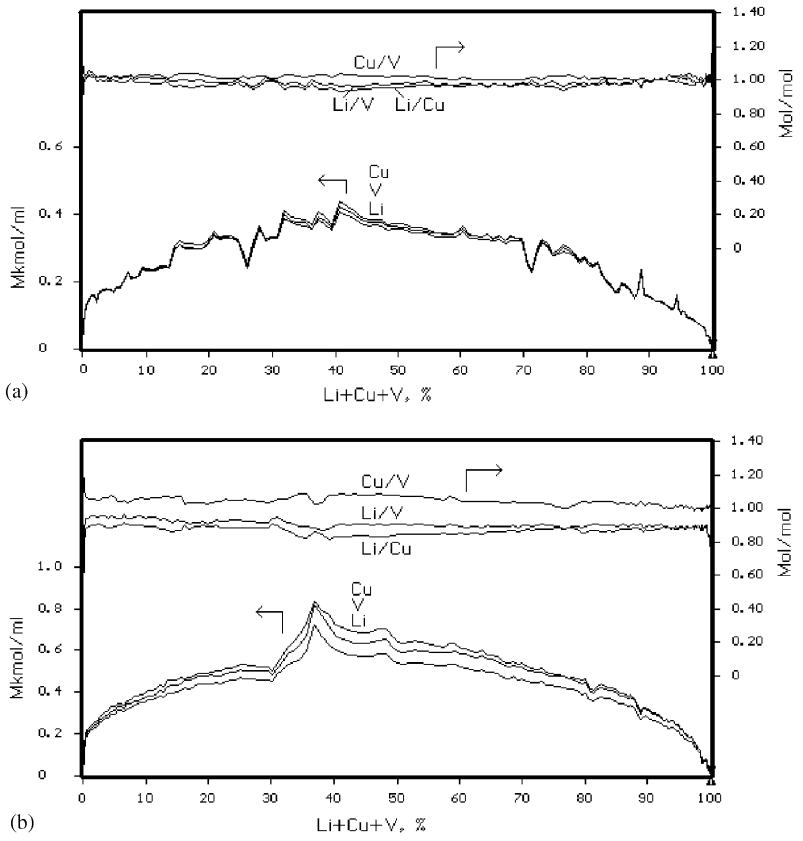

Fig. 3. Kinetic curves of elements dissolution and stoichiograms for a single-crystal sample 1(a) and 2(b). *Sample 1*—Li:V = 0.96 ± 0.05, Li:Cu = 0.95 ± 0.04, Cu:V = 0.99 ± 0.01 ($Li_{0.96}Cu_{0.99}V_{1.00}O_4$). *Sample 2*—Li:*V* = 0.93 ± 0.02, Li:Cu = 0.89 ± 0.02, Cu:V = 1.05 ± 0.01 ($Li_{0.93}Cu_{1.05}V_{1.00}O_4$).

ratio between the number of exactly stoichiometric and non-stoichiometric crystals is 1:4. According to the DD data (Fig. 3a), the averaged composition of sample 1 should be presented as $Li_{0.97}CuVO_4$. The observed composition variation is explained by varying parameters during the crystal growth (temperature, flux composition).

Crystals of sample 2 show another type of the DD pattern (Fig. 3b). The kinetic curves of Li, Cu and V diverse and all stoichiograms, being linear, differ from 1. Fig. 3b shows not only the lithium deficiency but also a copper over-stoichiometry, which was never observed for crystals of sample 1. This over-stoichiometric Cu, which varies from 1.01 to 1.04 for different crystals, reflects in this case the real composition of sample 2 rather than a statistical experimental error. In the total formula $Li_{1-x}Cu_{1+y}VO_4$, the x and the y values vary from 0.93 to 0.89 and from 1.01 to 1.04, respectively The average composition of sample 2 is $Li_{0.90}Cu_{1.03}VO_4$. As one can see, the Cu excess is not sufficient to compensate electrically the Li deficiency.

In contrast to single-crystalline samples, all powder samples have variable and non-linear stoichiograms. Their average values are characterized by large statistical errors (Fig. 4a–c). The figures show a spatial chemical inhomogeneity of powders due to variation in the composition of grains, and for sample 4 even a small quantity of an impurity phase with a composition of $Li_{1-x}VO_3$ ($x \approx 0.08$) was observed at the beginning of dissolution. Deviation of the stoichiograms from horizontal linearity during dissolution increases from sample 5 to samples 3 and 4, and their averaged compositions are found to be $Li_{0.98}Cu_{1.0}VO_4$, $Li_{0.87}Cu_{1.04}VO_4$, and $Li_{0.68}Cu_{1.00}VO_4$, respectively.

Despite the long annealing time and numerous grinding, all powder samples are characterized by a strong Li deficiency of the "$LiCuVO_4$" phase even in the presence of an Li-rich phase observed in sample 4. This could be explained by difficulties in achievement of equilibrium, taking into account the nonhomogeneity of powder grains found by the DD technique. However, the Li deficiency was observed also in single crystals, although they were grown from melts with a large excess of Li oxide, and the conditions facilitated the settle of the equlibrium. Probably, the Li deficiency is an equilibrium state of the "$LiCuVO_4$" phase at temperatures between 500°C and 600°C. A decrease in the Li deficiency was observed at lower temperature synthesis and almost stoichiometric composition was truly achieved for sample 5.

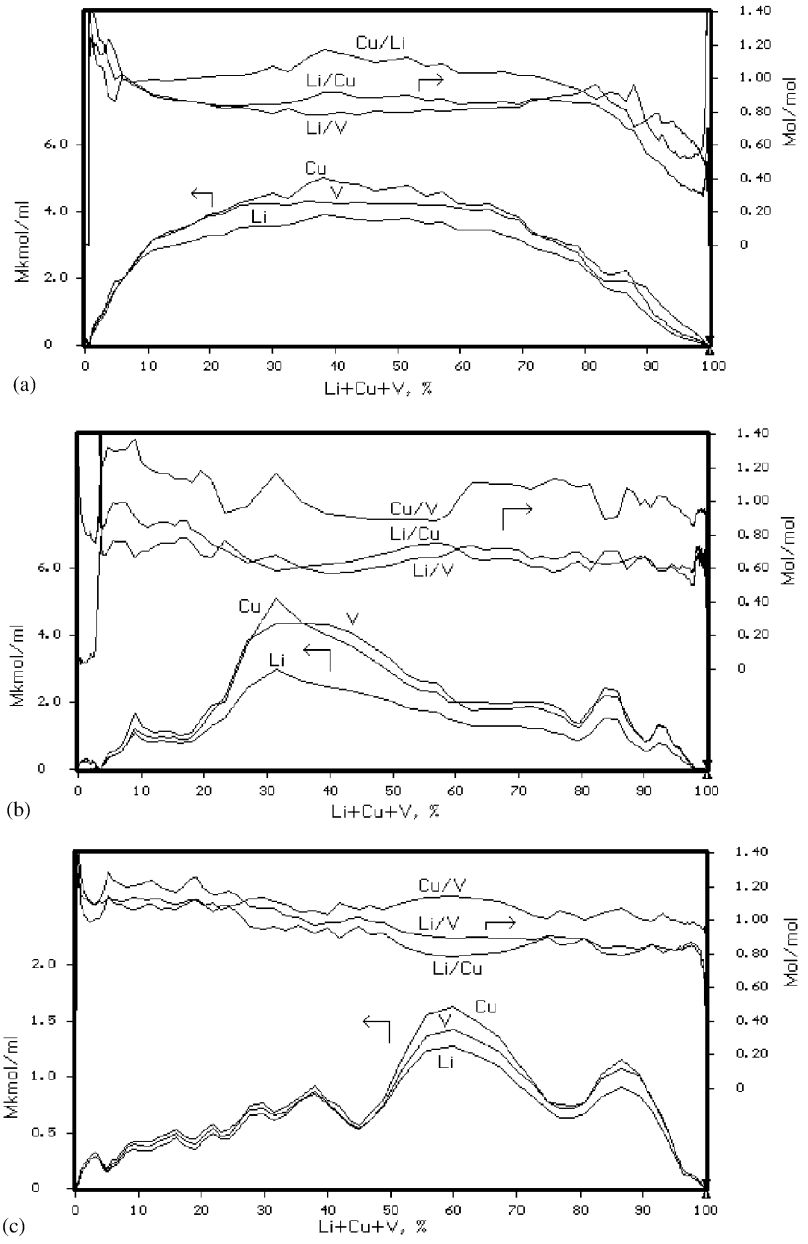

Fig. 4. Kinetic curves of element dissolution and stoichiograms for powder samples 3(a), 4(b) and 5(c). *Sample 3*—Li:$V = 0.87 \pm 0.04$, Li:Cu $= 0.84 \pm 0.10$, Cu:V $= 1.04 \pm 0.14$ ($Li_{0.87}Cu_{1.04}V_{1.00}O_4$). *Sample 4*—Li:V $= 0.68 \pm 0.23$, Li:Cu $= 0.67 \pm 0.12$, Cu:V $= 1.04 \pm 0.25$ (two phases: $Li_{0.68}Cu_{1.04}V_{1.00}O_4 + Li_{0.8}VO_3$ ~2%, are seen at the beginning of dissolution.). *Sample 5*—Li:V $= 0.98 \pm 0.30$, Li:Cu $= 0.98 \pm 0.23$, Cu:V $= 1.03 \pm 0.10$ ($Li_{0.98}Cu_{1.01}V_{1.01}O_4$).

Based on the composition data, samples 1–5 are classified into three groups: samples 1 and 5 have only a slight Li deficiency; samples 2 and 3 have a noticeable Li deficiency and a slight over-stoichiometry of copper; sample 4 has the highest Li deficiency without any excess of Cu. The real compositions are well correlated with the structural parameters (Table 2). The least lattice parameters were observed for samples 1 and 5 (the Li content is close to 1, no Cu excess) and the reflexes of the XRD patterns show clear doublets Cu$K\alpha_1$ and Cu$K\alpha_2$, confirming also the absence of structural cation disorder. The Cu over-stoichiometry of the $Li_{1-x}Cu_{1+y}VO_4$ samples results in a slight smearing of the reflex doublets, which means a structural cation disorder, and the broadening of these reflexes leads to an increase

Table 2
Parameters of the Curie–Weiss equation of samples 1–5

Sample	C (cm^3 K/mol)	$-\Theta$ (K)	μ_{eff} (μ_B)	T_N (K)
1	0.486 ± 0.002	23 ± 1	1.971	2,5
2	0.480 ± 0.004	26 ± 2	1.959	2,3
3	0.478 ± 0.003	25 ± 1	1.956	~4
4	0.484 ± 0.003	33 ± 1	1.968	2,1
5	0.424 ± 0.002	33 ± 1	1.84	2,8

in the lattice parameters. The highest Li deficiency without any Cu excess in sample 4 results in a distortion of the orthorhombic structure and this sample indeed differs structurally from all other samples.

3.3. XPS study

According to [6], the Li deficiency in $Li_{1-x}CuVO_4$ samples results in an appearance of non-Jahn–Teller Cu^{3+} ions in the 4*a* (Cu^{2+}) sites. The XPS study was performed to determine the formal oxidation state of Cu as well as of other elements in samples 1–5.

The V $2p_{3/2}$ and V $2p_{1/2}$ of all samples are practically identical (not shown). Both peaks, at 517 and 523.7 eV, were attributed according to [13] to V^{5+} ions. The Li 1*s* spectra (not shown) are identical for all samples too, except sample 3, where a splitting of the main peak into two components, with a higher and a lower BE, compared to other samples, appears. We explain this by the phase heterogeneity of the sample 3, which was confirmed by XRD through a higher diffusion background and by DD through the detection of the $Li_{1-x}VO_y$ impurity phase.

The O 1*s* and Cu 2*p* spectra of all samples are shown in Fig. 5. The O 1*s* peak, at about 530 eV, is typical for O^{2-} ions. There is practically no difference in the V spectra of all samples, but O/V ratio decreases slightly, going from sample 5 to 1, 2 and 3. For sample 4, this ratio decreases substantially compared to the other ones. This shows an oxygen non-stoichiometry of sample 4. A slight oxygen deficiency may be present also in other samples. Therefore, it is better to represent the composition of the substance by the formula $Li_{1-x}Cu_{1+y}VO_{4-z}$.

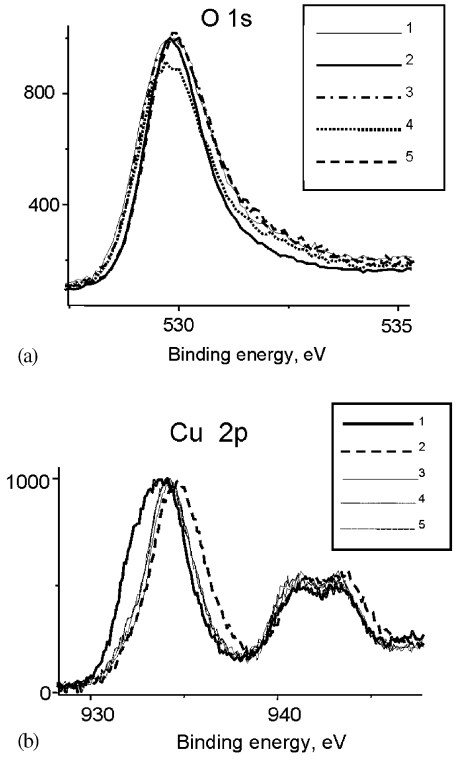

Fig. 5. O 1*s* (a) and Cu 2*p* (b) XPS spectra of samples 1–5.

The chemical shift of the Cu 2*p* BE from 933.5 to 934.1 eV in samples 1–5 is explained by an increase in the positive charge on copper in all samples compared with sample 1 (Fig. 5b). The Cu $2p_{3/2}$ peak at 933.5 eV was assigned to Cu^{2+}, which agrees well with the BE value of 933.6 eV for Cu^{2+} ions measured in CuO [14]. For other samples, the Cu 2*p* BE is higher, which is connected with an increase of its effective charge. The increase in the positive electron density of Cu ions is accompanied by an increase in the *c* parameters of samples 2–4 (see Table 2). This difference in BE and in the *c* parameters is especially pronounced for the single-crystalline samples 1 and 2. Despite the different Li deficiency of the powder samples 3–5, their Cu 2*p* peaks have equal BE of 934.1 eV, and they are placed between that of samples 1 and 2. XPS is a surface technique and, probably, the main reason of the similarity of all powder sample spectra is an identical composition of surface layers of grains, which is also confirmed by the DD data. Our XPS study confirmed the idea of compensation of Li deficiency by an increase in the charge of Cu ions [6]. However, we do not exclude a compensation of the Li deficiency also by the oxygen deficiency, which becomes primary for sample 4 with the strongly Li non-stoichiometry without the Cu excess.

3.4. Defect model of $Li_{1-x}Cu_{1+y}VO_{4-z}$

Let us now consider crystallochemical aspects of non-stoichiometry in $Li_{1-x}Cu_{1+y}VO_4$ samples. In the ideal $LiCuVO_4$ structure, the lithium and copper ions are located on the octahedral sites 4*d* and 4*a*, respectively (Fig. 1). The structural refinement of the samples with the compositions of $Li_{0.8-0.9}CuVO_{4-z}$ shows that an occupation of Li vacancies by Cu^{2+} and introduction of non-Jahn–Teller Cu^{3+} ions in the 4*a* copper sites lead to a decrease in the lattice parameter *c* in the low-temperature modification [6]. The increase in the parameter *c* with the Li deficiency in the high-temperature phase was explained by a larger copper occupancy on the 4*d* sites and a more disordered arrangement resulting in a larger Jahn–Teller distortion of the CuO_6 octahedra.

In our Li-non-stoichiometric samples 2, 3 and 4, an increase in the lattice parameter *c* is observed (the parameters *a* and *b* are less sensitive to the non-stoichiometry), despite the fact that the Cu effective charge increases, according to the XPS study. Therefore, we suggest another—than in [6]—scheme of the defect states for our non-stoichiometric samples. Cu^{2+} on the

4*d* sites (Cu_{Li}^{2+}) and vacancies in 4*d* (V_{Li}) are the reason for the increase in *c*. An occupation of the 4*a* sites by non-Jahn–Teller ions Li^{+} and Cu^{3+} (Li_{Cu}^{1+} and Cu_{Cu}^{3+}) as well as of the 4*d* sites by Cu^{3+} (with a somewhat smaller size than Li^{1+}) would lead to a decrease in *c*. For sample 2 with the averaged composition $Li_{0.90}Cu_{1.03}VO_{4-z}$, both the positive charge on copper (hence the Cu^{3+} concentration) and the *c* parameter are larger than that of sample 1 with the averaged composition $Li_{0.97}CuVO_{4-z}$. This means that Cu^{3+} ions occupy preferably 4*d* (Cu_{Li}^{3+}) rather than 4*a* positions (Cu_{Cu}^{3+}). The occupation of the LiO_6 octahedra by Cu^{3+} occurs almost without their contraction. Since the copper excess is too small to occupy all the Li vacancies, a possibility for an occupation of the empty 4*d* positions by Cu^{2+} from 4*a* sites appears. The appearance of Cu in 4*d* sites (Cu_{Li}^{2+}, Cu_{Li}^{3+}) and V_{Cu} in 4*a* sites introduce a more disordered arrangement in LiO_6 and CuO_6 octahedra for samples 2 and 3 compared with sample 1.

For sample 4, the high Li deficiency is accompanied by an oxygen non-stoichiometry, according to the XPS investigation and by the broken orthorhombic symmetry displayed as a splitting of the reflexes (Fig. 2). Only in sample 4 the structural phase transition described in [6] was observed.

The Li vacancies are the reason for the high superionic conductivity and an anomaly in the thermal conductivity in single-crystal samples 2, especially along the *a*- (Li chain) direction, as it was found recently [15–17]. These features are pronounced much weaker in single-crystal sample 1.

Although our XPS and DD measurements show that the excessive charge introduced by the Li non-stoichiometry is compensated by an excess of Cu, by a deficiency of oxygen and by an increase in the positive charge on Cu (holes localized on Cu), one more possibility should be considered. The holes in cuprates may be localized also on oxygen atoms. This case will be considered in the next section.

3.5. Magnetic properties

In all, 30–40 crystals were necessary for magnetic measurements contrary to the XRD, XPS, and DD techniques performing measurement with one crystal. Therefore, the interpretation of the magnetic properties of the crystalline samples 1 and 2 should base on their averaged compositions (see Section 3.2). The non-stoichiometric samples 1 and 2 differ one from another by a concentration of defects located in the Cu chains and outside. We consider spin-chain breaks resulting from either vacancies in the 4*a* positions or from a substitution by non-magnetic ions on the 4*a* Cu sites as well as Cu^{2+} or Cu^{3+} ions in the 4*d* sites as paramagnetic impurities. Cu^{3+} being in the 4*a* sites means a magnetic spin $S = 1$ impurity in the $S = 1/2$ chains.

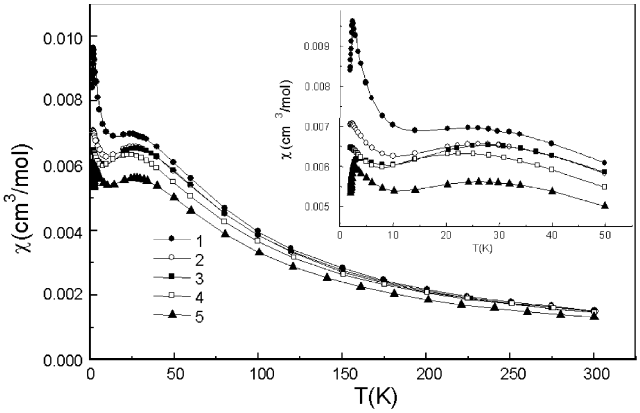

Fig. 6. Magnetic susceptibility of samples 1–5.

The temperature dependence of the magnetic susceptibility of samples 1–5 is shown in Fig. 6. The magnetic susceptibility goes through a broad maximum at about 25 K, then increases somewhat at 9 K and decreases sharply again at about 3 K. The latter feature is more pronounced for samples 1 and 5.

The $\chi(T)$ dependence for powder $LiCuVO_4$ samples was presented by many authors, who interpreted it to be typical for a quasi-one-dimensional magnetic system: at decreasing temperature, the system shows the short-range AF correlations in the Cu chains and then the three-dimensional antiferromagnetic ordering occurs at $T_N \sim 3$ K [2–5].

Our $\chi - T$ curves differ from earlier published ones measured on powders only in the case of samples 1, 2 and 5: they have rather high magnitude of upturn below 9 K and quite sharp maximum at ~ 3 K. The origin of the upturn below 9 K was explained most often by paramagnetic impurities [2–5], although an alternative explanation concerning a frustration through interchain interaction was suggested in [2]. We discuss here this upturn with respect to the defect states and chemical homogeneity of our samples (see Sections 3.2 and 3.4).

All samples obey a Curie–Weiss law in the temperature range of 80–300 K, with the parameters listed in Table 2. The μ_{eff} values obtained here are slightly higher comparing with the expected ones for the $Cu^{+2}E_g$ ground state in octahedral crystals field, which is equal to 1.93 μ_B, but they are close to those 1.88, 1.95, and 2.05μ_B measured by other authors for $LiCuVO_4$ [3–5].

The magnetic susceptibility can be fitted excellently within the $S = 1/2$ Heisenberg antiferromagnetic chain model, by taking into account a paramagnetic impurity Curie–Weiss term and temperature-independent magnetism:

$$\chi_M = \chi_{chain} + p\frac{0.375}{T - \theta_p} + \chi_{TIP}, \quad (1)$$

where the first term is given by the Bonner–Fischer numerical expression [18]:

$$\chi_{\text{chain}} = \frac{Ng^2\beta^2}{kT}\frac{A + Bx + Cx^2}{1 + Dx + Ex^2 + Fx^3} \quad \left(x = \frac{J}{kT}\right), \qquad (2)$$

with $A = 0.25$; $B = 0.14995$; $C = 0.30094$; $D = 1.9862$; $E = 0.68854$; $F = 6.0626$, and p is the paramagnetic impurity concentration with the spin $S = 1/2$. Optimal parameters of the model are given in Table 3, the fit is shown in Fig. 6 as solid lines.

As it follows from Table 3, the defect concentration decreases in the sample series $4>1>2>3>5$. This sequence contradicts our conclusion based on the results of the composition and the structural studies. According to the latter, the concentration of defects decreases in the $4>3>2>1>5$ sample series. To eliminate this contradiction, we analyzed in detail the low-temperature part of the $\chi(T)$ curves. It seems reasonable to analyze the $\chi(T)$ curves only for the single-crystal samples 1 and 2 as highly chemically homogeneous ones, according to DD. Actually, the powder samples 3 and 4 show a small magnitude of the upturn and the magnetic phase transition here takes place over a relatively wide temperature range. The spatial chemical inhomogeneity of the powder samples could explain such behavior. As for crystalline samples, sample 1 with the lowest Li deviation from the stoichiometry and, hence, with the highest perfection of the magnetic sublattice has a much higher magnitude of the upturn compared with that of sample 2. This finding excludes paramagnetic defects as the main reason of the upturn. The authors of [2] came to this conclusion, performing ESR measurements of powder $LiCuVO_4$, which did not reveal any additional paramagnetic signal below T_N. However, it is not the task of this work to analyze the system on the presence of Dzyaloshinskii–Moria interaction or staggered field effects, which have similar manifestation in the low-temperature magnetic susceptibility [19]. Here we should point out only that $LiCuVO_4$ appeared to be a strongly frustrated spin system. Recent neutron-scattering investigations on $LiCuVO_4$ showed that the strongest interaction along the chain is not between the nearest neighbors (NN), but between the next-nearest neighbors (NNN) [20]. The NN interaction (irrespective of whether AFM or FM) frustrates the main AFM NNN interaction. Taking the upturn as an intrinsic property of $LiCuVO_4$, a more complicated model than the Heisenberg spin chain should be developed to describe $LiCuVO_4$ as a strongly frustrated spin system.

Table 3
Parameters according to (1) for samples 1–5

Sample no.	P	θ_p (K)	g	J (K)	σ
1	0.054	−1.1	2.27	22.5	0.00131
2	0.041	−2.8	2.25	22.9	0.00103
3	0.034	−3.8	2.26	22.8	0.00102
4	0.159	−19.5	2.11	24.5	0.00033
5	0.0175	−4.4	2.12	23.9	0.000334

With increase in the Li non-stoichiometry, as it was established by XPS, the positive charge on the Cu ion increases. This should lead to a higher value of the Cu magnetic moment and, hence, of the magnetic susceptibility for samples with a higher Li deficiency. However, the opposite tendency is observed (if to exclude sample 5). This fact may be explained by formation of Zhang–Rice singlets [21]. Holes induced by Li non-stoichiometry may localize on the $2p$ orbital of oxygen. The spin of oxygen O(1) and that of copper Cu^{2+} couple antiferromagnetically, thus rendering the CuO_4 unit nonmagnetic. The magnetic susceptibility curves show that the localization of holes on oxygen predominates over the localization on Cu. The localization is strong and $LiCuVO_4$ remains electronically insulating.

4. Conclusion

It was shown that a non-stoichiometry of various degrees and types may be present in the series of $LiCuVO_4$ samples prepared by different techniques. The defects of the magnetic sublattice (Cu^{2+}) and its influence on the magnetic properties of $LiCuVO_4$ were considered based on the study of real stoichiometry and structure of the single-crystal and powder samples. For single crystals, it was shown that the upturn of $\chi(T)$ curves below 10 K could not be explained by defects; hence, an additional evidence was obtained to consider $LiCuVO_4$ as a strongly frustrated spin system. This feature of the $\chi(T)$ curves for the powders with their chemical spatial inhomogeneity is not pronounced. The Li non-stoichiometry is compensated partially by an oxygen deficiency. Not compensated positive charges (holes) are localized both on oxygen and copper ions, the former type of localization prevailing.

Acknowledgments

The work was performed in the framework of a Russian–German co-operation program and partially supported by the Integral project of SB RAS 88-2003, by 4.2 program of RAS, project 6-2003 and by the DFG Schwerpunktprogramm 1073. The authors would like to thank Mr. D. Naumov for the single-crystal X-ray measurements.

References

[1] M.A. Lafontaine, M. Leblanc, G. Ferey, Acta Crystallogr. C 35 (1989) 1205–1206.

[2] A.N. Vasil'ev, L.A. Ponomarenko, H. Manaka, I. Yamada, M. Isobe, Y. Ueda, Phys. Rev. B 64 (2001) 024419.
[3] A.N. Vasil'ev, et al., Physica B 284/288 (2000) 1619–1620.
[4] A.N. Vasil'ev, et al., JETP Lett. 69 (1999) 876–880.
[5] M. Yamaguchi, T. Furuta, M. Ishikava, J. Phys. Soc. Jpn. 65 (1996) 2998–3006.
[6] R. Kanno, Y. Kawamoto, Y. Takeda, M. Hasegava, O. Yamomoto, N. Kinomura, J. Solid State Chem. 96 (1992) 397–407.
[7] A.V. Prokofiev, D. Wichert, W. Assmus, J. Cryst. Growth 220 (2000) 345–350.
[8] V.V. Malakhov, Zh. Analit. Khim. 49 (1994) 349–360.
[9] V.V. Malakhov, J. Mol. Catal. A: Chem. 158 (2000) 143–148.
[10] V.V. Malakhov, J. Spectrochim. Acta Part B: Atom. Spectrosc. 58 (2) (2003) 373–386.
[11] J.C. Joubert, J.C. Grenier, A. Durif, C.R. Acad. Sci. 260 (1965) 2472–2475;
A. Durif, J.C. Grenier, J.C. Joubert, Tran-Qui-Duc. Bull. Soc. Fr. Miner. Crist. 89 (1966) 407–411.
[12] R. Kanno, Y. Takeda, M. Hasegawa, Y. Kawamoto, O. Yamamoto, J. Solid State Chem. 94 (1991) 319–328.
[13] P. Rozier, J. Galy, G. Chelkowska, H.-J. Koo, M.-H. Whangbo, J. Solid State Chem. 166 (2002) 382–388.
[14] H. Teikichi, Jpn. J. Appl. Phys. 26 (1987) l1596.
[15] L.S. Parfen'eva, A.I. Shelykh, I.A. Smirnov, A.V. Prokof'ev, W. Assmus, H. Misiorek, J. Mucha, A. Jezowski, I.G. Vasil'eva, Phys. Solid 45 (2003) 2093–2098.
[16] L.S. Parfen'eva, I.A. Smirnov, H. Misiorek, J. Mucha, A. Jezowski, A.V. Prokofiev, W. Assmus, Spinon thermal conductivity of –(CuO_2)-spin chains in $LiCuVO_4$, Phys. Solid State 46 (2) (2004) 357–363.
[17] L.S. Parfen'eva, A.I. Shelykh, I.A. Smirnov, A.V. Prokof'ev, W. Assmus, Electric conductivity and dielectric constant of the one dimensional superionic conductor $LiCuVO_4$, Phys. Solid State 46 (6) (2004) 1027–1029.
[18] O. Kahn, Molecular Magnetism, VCH, Weinheim, 1993, p. 380.
[19] E.E. Kaul, H. Rosner, V. Yushankhai, J. Sichelschmidt, R.V. Shpanchenko, C. Geibel, Phys. Rev. B 67 (2003) 174417.
[20] B. Gibson, R.K. Kremer, A.V. Prokofiev, W. Assmus, G. McIntire, Physica B (2004) (in press).
[21] F.C. Zhang, T.M. Rice, Phys. Rev. B 37 (1988) 3759–3761.